

Simulation of enzymatic cellular reactions complicated by phase separation

V. P. Zhdanov*

Department of Applied Physics, Chalmers University of Technology, 412 96 Göteborg, Sweden

and Boreskov Institute of Catalysis, Russian Academy of Sciences, Novosibirsk 630090, Russia

(Received 30 May 2000; revised manuscript received 11 September 2000; published 22 December 2000)

We present two-dimensional Monte Carlo simulations of enzymatic cellular reaction occurring via the Michaelis-Menten scheme in the case of attractive interactions between the reaction products. The model employed predicts phase separation in the cell provided that the reaction is relatively fast. The shape of the corresponding patterns varies from a few separate islands to a large patch located in the center of the cell. The fluctuations of the reaction rate during such regimes are found to be much higher than those predicted by the Poissonian distribution.

DOI: 10.1103/PhysRevE.63.011908

PACS number(s): 87.17.Aa, 05.70.Ln, 82.40.Bj, 87.16.-b

I. INTRODUCTION

In chemical reactions occurring far from equilibrium, spontaneous spatial self-organization is possible if reactant diffusion is coupled with chemical feedback. This seminal conclusion was drawn by Turing [1,2] in 1952. Since then, this phenomenon or, more specifically, reactant segregation and standing or traveling waves have attracted considerable attention from chemists, physicists, and biologists [3–6]. Traditionally, these processes are described by using the mean-field reaction-diffusion (MFRD) equations based on the conventional mass-action law. In particular, this approach (or simulations using lattice-gas automata [7] with similar rules) was used to analyze the pattern formation in individual cells [8–12] (for recent observations of traveling patterns in separate living cells, see Ref. [13]). Despite the available advances [7–13], the understanding of the mechanisms and kinetics of the spatiotemporal self-organization in cells is still a challenging problem. Its complexity has two counterparts. The first one is connected with a multitude of elementary reaction steps occurring in cells. Often, the steps are not well established and the information on their rate constants is limited or lacking. Under such circumstances, one is usually enforced to employ reduced generic reaction schemes with the corresponding MF or MFRD kinetic equations based on the mass-action law [11,14–16]. The second aspect of the problem under consideration is that the applicability of the mass-action law to the enzymatic cellular reactions is often questionable [17]. The reasons are as follows:

(i) Reactants are supplied into cells via external membranes. Thus, the cellular reactions occur in small confined volumes with the corresponding boundary conditions.

(ii) Cell structure is often highly inhomogeneous. For example, eukaryotic cells contain several specialized compartments separated by internal membranes [18].

(iii) The mass-action law is applicable to reactions of the Poissonian type. The internal dynamics of complex biological molecules or assemblies of molecules may however result in non-Poissonian effects [17,19]. In particular, due to

the complexity of the energy landscape of such molecules, the distribution of the reaction times may be broader than the Poissonian one (in other words, the average reaction time may be shorter than the variance about the mean).

(iv) Enzymatic reactions may be accompanied by phase separation of reactants due to attractive reactant-reactant interactions. If this is the case, the mean-field approximation is no longer applicable.

Our work is focused on factor (iv), i.e., we treat enzymatic cellular reactions complicated by phase separation of reactants. Concerning this subject, it is appropriate to note that in a more general context the patterns related to phase separation under the steady-state chemically reactive conditions were studied by Glotzer *et al.* [20]. Using Monte Carlo (MC) simulations, they explored the simplest $A \rightleftharpoons B$ reaction in a binary mixture during spinodal decomposition. Employing the Kawasaki dynamics to exchange nearest-neighbor (NN) molecules, Glotzer *et al.* obtained that a combination of the reaction and spinodal decomposition results in the formation of well-developed labyrinthine structures (for related more recent studies, see Ref. [21]). There are also a few simulations of catalytic reactions occurring on a solid surface and accompanied by phase separation resulting from attractive adsorbate-adsorbate interactions (see the review in Ref. [22]). Experimental observations of phase separation in 2D catalytic reactions are numerous [23,24], but as a rule the reports on this phenomenon are connected rather with adsorbate-induced surface restructuring than with attractive interactions between adsorbed particles (see the reviews [23,25] and recent simulations [26]). Phase separation in cellular reactions catalyzed by enzymes was never analyzed before, because direct experimental data on such reaction regimes are lacking. There are, however, general theoretical arguments and indirect experimental data indicating that this phenomenon may be important in cells.

Appealing to general theory, we may recall that one of the main functions of enzymes is to cleave long biological molecules in shorter fragments. Such fragments often contain parts which are more hydrophilic or hydrophobic compared to the initial species. The hydrophobic-hydrophobic interaction is usually attractive. The hydrophilic-hydrophilic interaction may be attractive as well. Thus, both these interactions may result in reactant aggregation.

Concerning experiment, we may refer to protein adsorp-

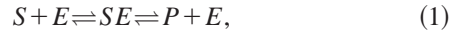
*Electronic address: zhdanov@catalysis.nsk.su

tion. In the past (about ten years ago), the general opinion was that aggregation of adsorbed proteins is a rare effect (see, e.g., the reviews in Ref. [27]). Then, with the development of new experimental techniques, it has, however, been found that proteins, adsorbed at a gas-liquid interface that is clean or covered by a lipid monolayer, often form mesoscopic one-molecule thick islands with sizes up to $100 \mu\text{m}$ (for a review of proteins which may undergo 2D phase separation, see Refs. [28,29]). One of the best examples here is 2D crystallization of streptavidin at a biotinylated lipid layer [30]. In this case, the formation of large 2D islands (up to $\sim 100 \mu\text{m}$) occurs within minutes across a pH range from 1.5 to 11 (with increasing pH, the streptavidin structures varies from needle-shaped crystals with P1 and/or P2 symmetry at $1.5 \leq \text{pH} \leq 5$ to more isotropic X, H or rectangular C222 islands at $7 \leq \text{pH} \leq 11$). In analogy with protein adsorption, one may expect that phase separation in cells is more common than it is considered now.

Taking into account the arguments above, we believe that exploring phase separation in enzymatic cellular reactions merits attention, especially if one takes into account that this problem is of interest from a physical point of view.

II. MODEL

In cells, enzymatic catalytic reactions usually run via a set of elementary steps occurring via the Michaelis-Menten scheme [14,15,31],



where S is the substrate, E is the enzyme, SE is the substrate-enzyme complex, and P is the product. In the case of cleavage of long chains, P should actually be replaced by two molecules. To not obscure the main message, we treat below the simplest generic case when the reaction runs via the steps,



including the formation of SE and *rapid irreversible* transition to $P + E$. The latter step is assumed to be realized immediately after formation of SE . The concentration of SE is accordingly considered to be negligibly low.

In our MC simulations, the cell is represented by a 2D $L \times L$ square lattice. Each lattice site can be occupied only by one particle (S , P , or E). Diffusion of S and P occurs via jumps to NN vacant sites. Both processes are assumed to be relatively rapid and run with the same rate. (In principle, in analogy with the Ising model, one could include the S - P exchange acts into the reaction scheme. It might slightly facilitate phase separation. In cellular reactions, the exchange processes are, however, hardly possible.) Diffusion of E is neglected, because the molecular weight of enzymes is considered to be larger than those of the reactants. Reaction (2) is realized between S and E particles located in NN sites.

In cells, the reactant supply and removal usually occur via special membrane proteins. In our present simulations, the distribution of membrane proteins is considered to be homogeneous, so that there are no preferable patches for supply or

removal of reactants. In this case, there is no need to treat membrane proteins explicitly. Instead, we may simply prescribe to the boundary sites the effective probabilities of reactant supply or removal.

To incorporate phase separation into the scheme above, the interaction between NN P particles is considered to be attractive, $\epsilon_1 < 0$. The other interactions are neglected. In this case, the critical temperature, given by the well-known Onsager equation, is $T_c = 0.567 |\epsilon_1| / k_B$.

With particle-particle interactions, the rate constant of an elementary rate process for a given arrangement of particles can be represented as [32]

$$k_i = k_\circ \exp[-(\epsilon_i^* - \epsilon_i)/k_B T], \quad (3)$$

where k_\circ is the rate constant corresponding to the case when the sites adjacent to the particles participating in the process are vacant, ϵ_i and ϵ_i^* are the lateral interactions (in the initial and activated states) of these particles with adjacent particles, and i is the subscript characterizing the arrangement.

In MC simulations, the probabilities of elementary steps should be dimensionless. Practically, this means that the rate constants of various steps should be normalized to the rate constant of the fastest step so that the probability of this step is equal to unity [33]. In our simulations, the fastest processes are considered to be S and P diffusion. The probabilities of S jumps to NN vacant sites, $p_S^{\text{dif}} = 1$, and S supply in and removal out of the cell, $p_S^{\text{in}} < 1$ and $p_S^{\text{out}} < 1$, are assumed to be independent of the arrangement of adjacent particles, because for S particles $\epsilon_i^* = \epsilon_i = 0$. The effect of particle-particle interactions on the probability of reaction (2), $p_r \leq 1$, is neglected as well. For the dimensionless probabilities

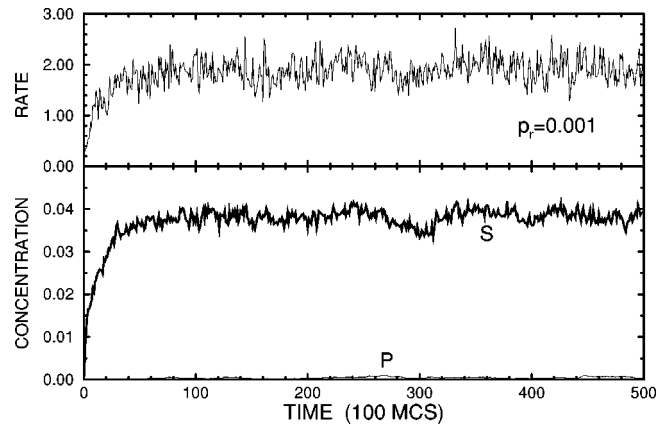


FIG. 1. S and P concentrations (per site) and reaction rate (P molecules per site per MCS) as a function of time for $\epsilon_1/k_B T = -3$, $L = 100$, $N_E = 50$, $p_S^{\text{in}} = 0.01$, $p_S^{\text{out}} = 1$, $p_P^{\text{out}} = 0.1$, and $p_r = 0.001$. The interval between the data points is 100 MCS. The reaction rate is calculated as the average over 100 MCS. [In this case, the steady-state reaction rate is about 2. This corresponds to the formation of about 200 P molecules during 100 MCS. According to the Poissonian distribution, the root-mean-square deviation (RMSD) from this number should be about 15. The corresponding RMSD from the reaction rate is about 0.15. The latter value is comparable with the average amplitude of fluctuations of the reaction rate.]

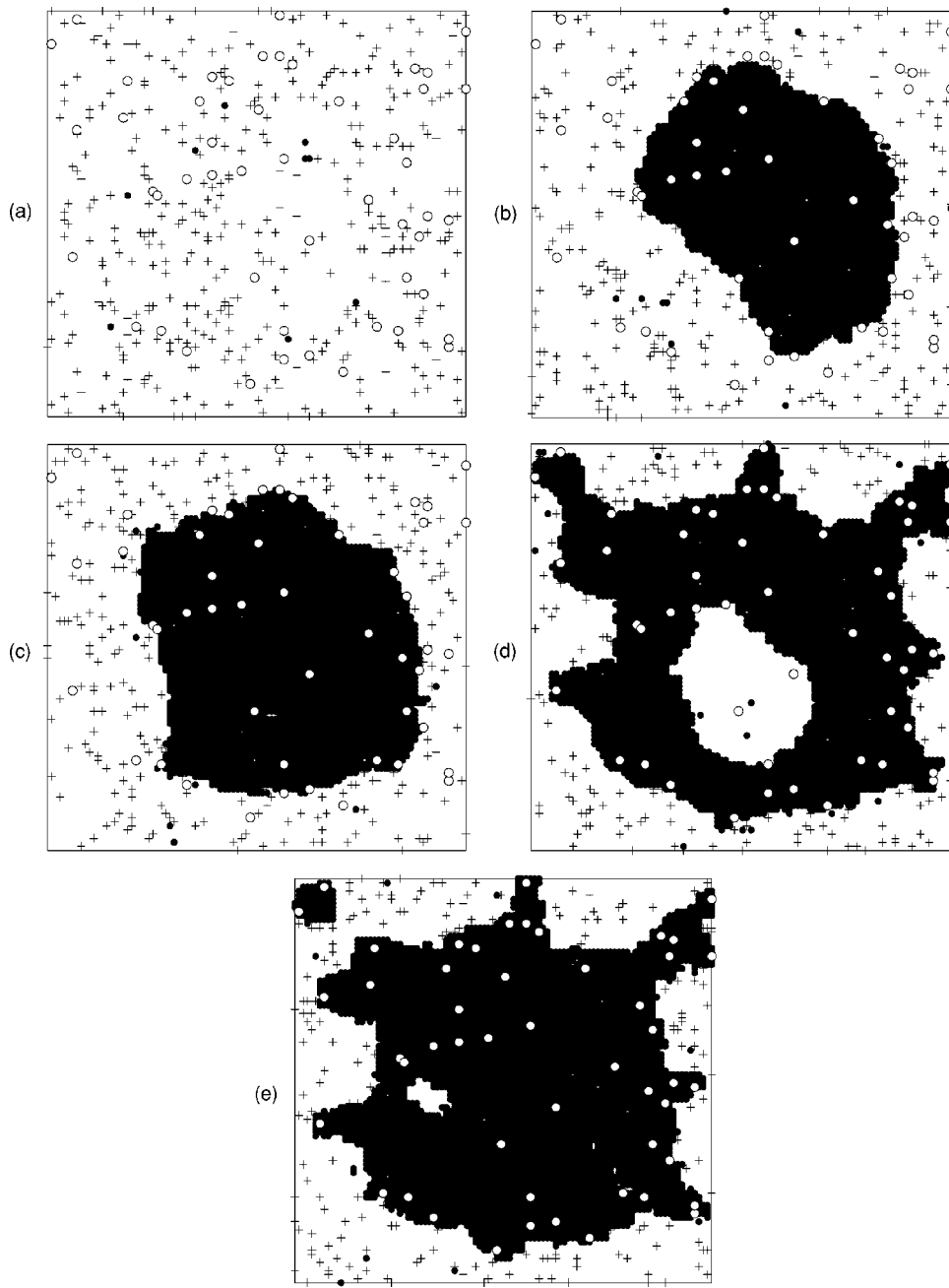


FIG. 2. S (plus signs), P (filled circles), and E (open circles) particles on the 100×100 lattice at $t = 10^7$ MCS for $p_r = 0.001$ (a), 0.007 (b), 0.01 (c), 0.1 (d), and 1 (e). The values of the other parameters are the same as in Fig. 1.

of P jumps to NN vacant sites and out of the lattice, we use the so-called initial-state dynamics [22,32], corresponding to $\epsilon_i^* = 0$, i.e.,

$$p_n^{\text{dif}} = \exp(\epsilon_1 n / k_B T), \quad (4)$$

$$p_n^{\text{out}} = p_{\text{out}} \exp(\epsilon_1 n / k_B T), \quad (5)$$

where n is the number of NN P particles (note that $p_n^{\text{dif}} = 1$ for $n = 0$; this means that the maximum rate of P diffusion is the same as that of S diffusion). This is the simplest physically reasonable dynamics compatible with the detailed balance principle. If necessary, one can use another dynamics for P diffusion. For the reaction under consideration, the

qualitative conclusions are expected to be independent of the details of the dynamics as long as it satisfies the detailed balance principle.

III. ALGORITHM OF MC SIMULATIONS

To simulate the reaction under consideration, we first distribute N_E E particles on the $L \times L$ lattice at random. Then, we choose randomly sites on the lattice and realize elementary processes involved into the game as follows:

(i) If the site chosen is vacant, there are three options depending on its location. For the vacant site located inside the $L \times L$ lattice, the trial ends. The vacant site located on the boundary is occupied by S with the probability p_S^{in} . The corner vacant site is occupied by S with the probability $2p_S^{\text{in}}$,

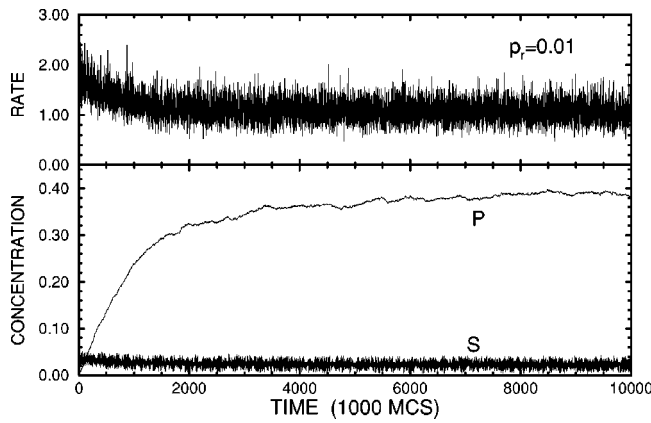


FIG. 3. S and P concentrations (per site) and reaction rate (P molecules per site per MCS) as a function of time for $p_r=0.01$ (the values of the other parameters are the same as in Fig. 1). The interval between the data points is 1000 MCS. The reaction rate is calculated as the average over 100 MCS.

because such site has two sides contacting the sites located outside the $L \times L$ lattice. (The filling of vacant boundary sites by S mimics S supply into the cell via the external membrane.)

(ii) If the chosen site (site 1) is occupied by S , one of the NN sites (site 2) is selected at random. If site 2 is vacant and located on the $L \times L$ lattice, S is replaced from site 1 to site 2 (this step mimics S diffusion). If site 2 is occupied by E , S is replaced by P with the probability p_r [this step mimics reaction (2)]. If site 2 is outside the $L \times L$ lattice (this is possible if site 1 is located on the boundary), S is removed from site 1 with the probability p_S^{out} (this step mimics S jumps from the cell). If site 2 is occupied by S or P , S remains in site 1.

(iii) If the chosen site (site 1) is occupied by P , one of the NN sites (site 2) is selected at random. If site 2 is vacant and located on the $L \times L$ lattice, P is replaced from site 1 to site 2 with the probability p_P^{dif} given by Eq. (4) (this step mimics P diffusion). If site 2 is located outside the $L \times L$ lattice, P is removed from site 1 with the probability p_P^{out} defined by Eq. (5) (this step mimics P jumps from the cell). If site 2 is occupied, P remains in site 1.

(iv) If the site chosen is occupied by E , the trial ends.

Initially (at $t=0$), the lattice is considered to be free of S and P . Time is calculated in MC steps (MCS). 1 MCS corresponds to $L \times L$ attempts to realize one of the rate processes. The kinetics were run up to $t=10^7$ MCS. Such a duration of runs was proved to be sufficient in order to reach the steady-state reaction regime.

IV. MEAN-FIELD EQUATIONS

To rationalize the results of MC simulations, it is instructive first to present the conventional mean-field equations describing the time dependence of the number of S and P particles on the lattice, N_S and N_P , in the case when the reaction is so slow that phase separation and concentration gradients are negligible. To obtain the equation for N_P , we note that the rate of S supply into the lattice is given by $4Lp_S^{\text{in}}$, where $4L$ is the length of boundaries. The rate of S

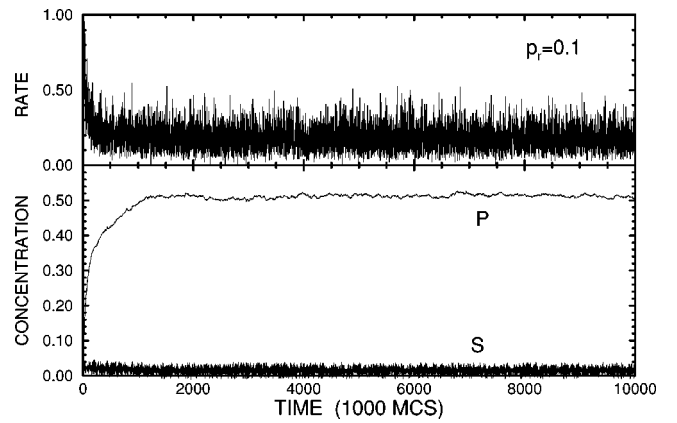


FIG. 4. As Fig. 3 for $p_r=0.1$.

jumps out of the lattice is $(p_S^{\text{out}}/L)N_S$ [this is a product of the length of boundaries, $4L$, the jump probability, $p_S^{\text{out}}/4$ (p_S^{out} is divided by 4, because the direction of jumps is chosen at random), and the concentration (per site) of S particles, N_S/L^2]. The reaction rate is represented as $p_r(N_E/L^2)N_S$, where N_E/L^2 is the E concentration (per site). Thus, we have

$$dN_S/dt = 4Lp_S^{\text{in}} - (p_S^{\text{out}}/L)N_S - (p_r/L^2)N_E N_S. \quad (6)$$

For the P particles, one can obtain in analogy

$$dN_P/dt = -(p_P^{\text{out}}/L)N_P + (p_r/L^2)N_E N_S. \quad (7)$$

The equations above hold provided that the reaction is slow. This means that the third term in the right-hand part of Eq. (6) can be neglected. In this approximation, the steady-state reaction regime is described as

$$N_S = 4L^2 p_S^{\text{in}}/p_S^{\text{out}}, \quad (8)$$

$$N_P = \frac{4Lp_r p_S^{\text{in}} N_E}{p_P^{\text{out}} p_S^{\text{out}}}. \quad (9)$$

According to Eq. (9), the P concentration per site is given by

$$c_P \equiv N_P/L^2 = \frac{4p_r p_S^{\text{in}} N_E}{L p_P^{\text{out}} p_S^{\text{out}}}. \quad (10)$$

On the other hand, the critical P concentration for phase separation is defined by the Onsager equation,

$$c_P^c = \{1 - [1 - (\text{sh}(\epsilon_1/2k_B T))^{-4}]^{-1/8}\}/2. \quad (11)$$

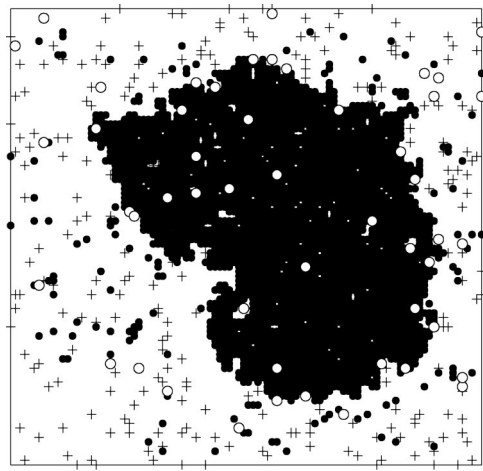
Phase separation is negligible if

$$c_P < c_P^c. \quad (12)$$

This condition is fulfilled provided that p_r [in Eq. (10)] is relatively small.

V. RESULTS OF SIMULATIONS

Our model contains the following parameters: ϵ_1 , L , N_E , p_r , p_S^{in} , p_S^{out} , and p_P^{out} . To illustrate the effect of phase sepa-

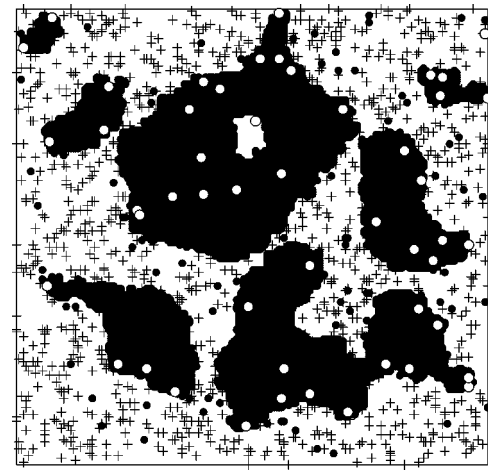
FIG. 5. As Fig. 2(d) for $\epsilon_1/k_B T = -2$.

ration on the reaction kinetics, we use $N_E = 50$, $p_S^{\text{in}} = 0.01$, $p_S^{\text{out}} = 1$, and $p_P^{\text{out}} = 0.1$ (with these parameters the S transport in and out of the cell and the P removal from the cell are relatively fast). The bulk of simulations was executed for $L = 100$ and $\epsilon_1/k_B T = -3$. The reaction probability p_r was varied in a wide range in order to show the transition from the case when phase separation is negligible to the situation when phase separation is significant.

The reaction kinetics for $p_r = 0.001$ are exhibited in Fig. 1. In this case, the P concentration is small and accordingly phase separation is negligible [Fig. 2(a)]. Under such circumstances, the transition to the steady-state regime is controlled by S diffusion. This process is relatively rapid. In particular, the steady state is reached already at $t = 10^4$ MCS (for this reason, we show the reaction kinetics only for $t \leq 5 \times 10^4$ MCS). The steady-state S concentration (per site), $c_S \equiv N_S/L^2$, is close to 0.04 as expected from Eq. (8). The fluctuations in the reaction rate are close to those predicted by the Poissonian distribution.

Phase separation starts at $p_r \approx 0.007$. First, the P phase is located in the center of the cell [see Fig. 2(b) for $p_r = 0.007$]. The P aggregation near the cell boundaries is not favorable because the P concentration in the latter region is small. With increasing p_r up to 0.01, the size of the P -phase region slightly increases [Fig. 2(c)]. With further increase of p_r , the P -phase region becomes circular [see Fig. 2(d) for $p_r = 0.1$]. For the maximum reaction rate, $p_r = 1$, almost the entire cell is filled by P [Fig. 2(e)].

Typical reaction kinetics complicated by P aggregation are shown in Figs. 3 and 4 for $p_r = 0.01$ and 0.1. In both cases, the time scale characterizing the transition to the steady-state regime is much longer than that corresponding to the situation when there is no P aggregation (Fig. 1),

FIG. 6. As Fig. 2(d) for $L = 200$.

because the process is limited by the slow growth of P islands. The fluctuations of the reaction rate are much higher compared to those expected on the basis of the Poissonian distribution, because in addition to fluctuations of S particles the number of enzymes really participating in the reaction fluctuates as well (a considerable part of enzymes is blocked by P molecules and accordingly does not participate in the reaction).

Finally, we show the P patterns predicted for higher temperature (Fig. 5 for $\epsilon_1/k_B T = -2$) and a larger lattice size (Fig. 6 for $L = 200$). In the former case, the boundaries of the P patch are much more disordered compared to those observed for $\epsilon_1/k_B T = -3$ (Fig. 2). With increasing L (Fig. 6), the average E concentration becomes lower and the conditions for the P aggregation are fulfilled only locally. For this reason, the P particles form a few islands.

VI. CONCLUSION

Employing the generic 2D model of enzymatic cellular reactions accompanied by reactant phase separation, we have shown that this phenomenon is possible if the reaction is relatively fast. The shape of the patterns of a new phase may vary from a few separate islands to a large patch located in the center of the cell. In real cells, the conditions for phase separation are expected to hold only in rare cases (in fact, phase separation may destroy normal regulation in the cell). Identification of such cases is of interest from the point of view of general theory of cellular reactions and statistical physics.

ACKNOWLEDGMENTS

The author thanks B. Kasemo for useful discussions. The financial support for this work was obtained from the Waernska Guest Professorship Fund at Göteborg University.

[1] A.M. Turing, *Philos. Trans. R. Soc. London, Ser. B* **327**, 37 (1952).
[2] B.R. Johnson and S.K. Scott, *Chem. Soc. Rev.* **25**, 265 (1996).
[3] *Diffusion Processes: Experiment, Theory, Simulations*, edited

by A. Pekalski (Springer, Berlin, 1994).
[4] *Chemical Waves and Patterns*, edited by R. Kapral and K. Showalter (Kluwer, Dordrecht, 1994).
[5] D. Walgraef, *Spatio-Temporal Pattern Formation* (Springer,

Berlin, 1996).

- [6] A. De Wit, *Adv. Chem. Phys.* **109**, 435 (1999).
- [7] B. Hasslacher, R. Kapral, and A. Lawniczak, *Chaos* **3**, 7 (1993).
- [8] M. Herschkowitz-Kaufman and G. Nicolis, *J. Chem. Phys.* **56**, 1890 (1972).
- [9] A. Goldbeter, *Proc. Natl. Acad. Sci. U.S.A.* **70**, 3255 (1973).
- [10] P. Marmillot, J.-F. Hervagault, and G.R. Welch, *Proc. Natl. Acad. Sci. U.S.A.* **89**, 12 103 (1992).
- [11] A. Goldbeter, *Biochemical Oscillations and Cellular Rhythms* (Cambridge University Press, Cambridge, 1996).
- [12] V.P. Zhdanov, *Phys. Chem. Chem. Phys.* **22**, 5268 (2000).
- [13] H.R. Petty, R.G. Worth, and A.L. Kindzelskii, *Phys. Rev. Lett.* **84**, 2754 (2000), and references therein.
- [14] H. Gutfreund, *Kinetics for Life Sciences* (Cambridge University Press, Cambridge, 1995).
- [15] C.D. Varfolomeev and K.G. Gurevich, *Biokinetics* (Fiar, Moscow, 1999).
- [16] M. Bier, B.M. Bakker, and H.V. Westerhoff, *Biophys. J.* **78**, 1087 (2000), and references therein.
- [17] B. Alberts, *Cell* **92**, 291 (1998).
- [18] B. Alberts, D. Bray, J. Lewis, M. Raff, K. Roberts, and J.D. Watson, *Molecular Biology of the Cell* (Garland, New York, 1994).
- [19] H. Frauenfelder, P.G. Wolynes, and R.H. Austin, *Rev. Mod. Phys.* **71**, S419 (1999).
- [20] S.C. Glotzer, D. Stauffer, and N. Jan, *Phys. Rev. Lett.* **72**, 4109 (1994).
- [21] D. Carati and R. Lefever, *Phys. Rev. E* **56**, 3127 (1997); S. Puri and H.L. Frisch, *Int. J. Mod. Phys. B* **12**, 1623 (1998); S. Toxvaerd, *Comput. Phys. Commun.* **122**, 251 (1999), and references therein.
- [22] V.P. Zhdanov, *Surf. Sci.* **392**, 185 (1997).
- [23] R. Imbihl and G. Ertl, *Chem. Rev.* **95**, 697 (1995).
- [24] H.H. Rotermund, *Surf. Sci. Rep.* **29**, 265 (1997).
- [25] M. Gruyters and D.A. King, *J. Chem. Soc., Faraday Trans.* **93**, 2947 (1997).
- [26] V.P. Zhdanov, *Phys. Rev. E* **59**, 6292 (1999).
- [27] *Proteins at Interfaces II*, edited by T.A. Horbett and J.L. Brash (ACS, Washington, 1995).
- [28] J.S. Erickson, S. Sundaram, and K.J. Stebe, *Langmuir* **16**, 5072 (2000).
- [29] V.P. Zhdanov and B. Kasemo, *Proteins* **40**, 539 (2000).
- [30] M.T. Yatcilla, C.R. Robertson, and A.P. Gast, *Langmuir* **14**, 497 (1998).
- [31] C. Branden and J. Tooze, *Introduction to Protein Structure* (Garland, New York, 1999).
- [32] V.P. Zhdanov, *Elementary Physicochemical Processes on Solid Surfaces* (Plenum, New York, 1991).
- [33] K. Binder, in *Monte Carlo Methods in Statistical Physics*, edited by K. Binder (Springer, Berlin, 1979), p. 1.